Workflow for Zoeppritz AVO Inversion to Estimate Seismic Anisotropy, Geomechanical Properties and TOC of Shale: Case Study of Avalon Shale, Delaware Basin*

Un Young Lim[1], Nurul Kabir[1], and Richard L. Gibson Jr.[1]

Search and Discovery Article #42416 (2019)**
Posted August 5, 2019

*Adapted from oral presentation given at 2019 AAPG Annual Convention and Exhibition, San Antonio, Texas, May 19-22, 2019

[1]Texas A&M University, College Station, Texas (luykms@tamu.edu)

Abstract

Reliable estimation of geomechanical properties (i.e. Young's modulus and Poisson's ratio) and total organic carbon (TOC) content of shale provides important constraints to guide petroleum production by identifying abundant organic sweet spots and locations for effective hydraulic fracturing. However, most conventional amplitude variation with offset (AVO) inversions cannot properly estimate the properties, since the inversions are developed based on linear approximations of Zoeppritz equations assuming weak contrasts and seismic isotropy. Organic-rich shale formations are, however, often anisotropic. In order to overcome limitations of the conventional methods, we propose a workflow to estimate seismic anisotropy and geomechanical properties of organic-rich shale. It is based on analyses of an AVO inversion with full Zoeppritz solutions mainly for P-wave reflection amplitudes.

The anisotropy of the model shale is related to the kerogen volume fraction values using measured well logs and laboratory data for the Avalon Shale in the Delaware Basin. By applying inversion tests, we determine behaviors of the AVO inversion solutions developed for isotropic media when the target shale formation instead has seismic anisotropy related to organic content. These tests show that the inversion accurately determines horizontal P-wave and S-wave velocities and underestimates density when a far angle range is applied with input data. When the angle range is small, the inversion can obtain reliable vertical velocities, and correct density. Therefore, seismic anisotropy of the model can be estimated by comparing these inverted horizontal and vertical velocities. In addition, geomechanical properties of the model are also reliably determined in both

horizontal and vertical directions. We also estimate organic carbon content of the Avalon Shale in Delaware Basin from density values obtained by an amplitude variation with offset (AVO) inversion. The estimation is based on an empirical relationship between kerogen volume fraction and density of the shale.

Selected References

Banik, N.C., M.S. Egan, et al., 2012, Effects of vti anisotropy on shale reservoir characterization: Presented at the SPE Middle East Unconventional Gas Conference and Exhibition, Society of Petroleum Engineers.

Barclay, F., A. Bruun, K.B. Rasmussen, J.C. Alfaro, A. Cooke, D. Cooke, D. Salter, R. Godfrey, D. Lowden, S. McHugo, et al., 2008, Seismic inversion: Reading between the lines: Oilfield Review, v. 20, p. 42-63.

Burger, J., and G. Chavent, 1979, Identification de param tres r partis dans les quations aux d riv es partielles: RAIRO, v. 13, p. 115-126.

Castagna, J.P., and M. Backus, 1993, AVO analysis - tutorial and review: Offset-dependent reflectivity: Theory and practice of AVO analysis: SEG Investigations in Geophysics, p. 3-36.

Fatti, J.L., G.C. Smith, P.J. Vail, P.J. Strauss, and P.R. Levitt, 1994, Detection of gas in sandstone reservoirs using AVO analysis: A 3-D seismic case history using the Geostack technique: Geophysics, v. 59, p. 1362-1376.

King, M.S., 1964, Wave velocities and dynamic elastic moduli of sedimentary rocks: PhD thesis, University of California, Berkeley.

Lavaud, B., N. Kabir, and G. Chavent, 1999, Pushing avo inversion beyond linearized approximation: Journal of Seismic Exploration, v. 8, p. 279-302.

Lim, U.Y., R. Gibson, N. Kabir, and D. Zhu, 2017, Inference of geomechanical properties of shales from avo inversion based on the Zoeppritz equations, in SEG Technical Program Expanded Abstracts 2017: Society of Exploration Geophysicists, p. 728-732.

Lim, U.Y., N. Kabir, and R.L. Gibson Jr, 2018, Horizontal-velocity estimation from pp-and ps-joint avo inversion based on Zoeppritz equations: Eagle ford case study, SEG Technical Program Expanded Abstracts 2018: Society of Exploration Geophysicists, p. 2422-2426.

Ruger, A., 1997, P-wave reflection coecients for transversely isotropic models with vertical and horizontal axis of symmetry: Geophysics, v. 62, p. 713-722.

Thomsen, L., 1986, Weak elastic anisotropy: Geophysics, v. 51, p. 1954-1966.

Wiggins, R., G. Kenny, and C. McClure, 1983, A method for determining and displaying the shear-velocity reflectivities of a geologic formation.

Zoeppritz, K., 1919, On the reflection and penetration of seismic waves through unstable layers: G¨ottinger Nachrichten, I, p. 66-84.

ACE 2019 AAPG ANNUAL CONVENTION & EXHIBITION
19-22 May • San Antonio, Texas

GEOLOGY AND GEOPHYSICS
TEXAS A&M UNIVERSITY

Workflow for Zoeppritz PP-AVO inversion to estimate seismic anisotropy, geomechanical properties, and TOC of shale: Case study of Avalon shale, Delaware Basin

Un Young Lim*, Nurul Kabir, and Richard L. Gibson

May 20, 2019

Berg-Hughes Center for Petroleum and Sedimentary Systems
Department of Geology and Geophysics, Texas A&M University

Table of contents

Research Objective

Research Objective and Contributions

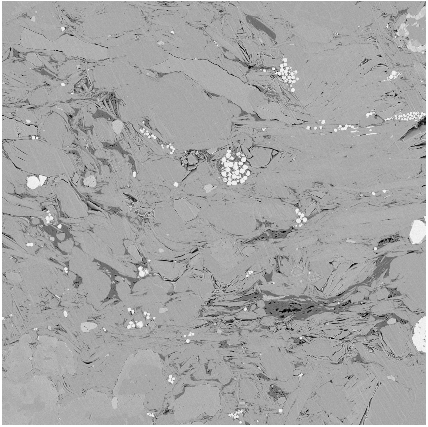

A Scanning Electron Microscope (SEM) image of shale, provided by Dr. Gibson

- Research Objective
  - Completion quality of unconventional shale reservoir
- Method
  - Nonlinear Zoeppritz AVO inversion
  - Workflow based on inversion results
  - Empirical relationship between ρ and TOC
- Contributions
  - Seismic anisotropy
  - Geomechanical properties (e.g., E, and ν)
  - Organic abundance (i.e. TOC) of shale

Method: Nonlinear AVO inversion based on Zoeppritz equations

Amplitude Variation with Offset (AVO) inversion

- Amplitude Variation with Offset (AVO) inversion
  - to estimate elastic properties of target layers (e.g., AI, SI, V_P, V_S, and ρ) [Castagna and Backus, 1993].
  - by minimizing the error between observed and modeled AVOs

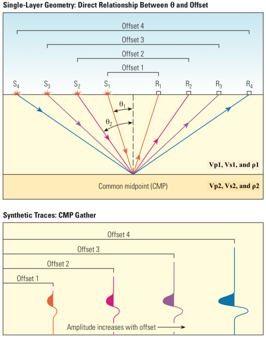

Modified from [Barclay et al., 2008]

$$E(x) = \frac{1}{2}\sum_{i=1}^{N_{obs}} \|R_i^c(x) - R_i^m\|^2, \tag{1}$$

where

R_i^m: observed reflectivity at θ_i

R_i^c: modeled reflectivity at θ_i

N_{obs}: number of observations (θ_i)

x: model parameters, V_{P1}, V_{P2}, V_{S1}, V_{S2}, ρ_1, and ρ_2

Research Motivation: Limitation of conventional AVO methods

- Conventional AVO methods: linearized approximations of Zoeppritz eq.
- Weak contrast & Isotropy
- cf) [Rüger, 1997] (Weak anisotropy & Weak contrast)

ex1: Isotropy & Strong contrast

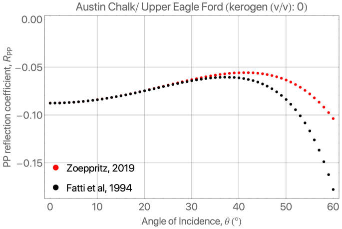

ex2: Strong anisotropy & Weak contrast

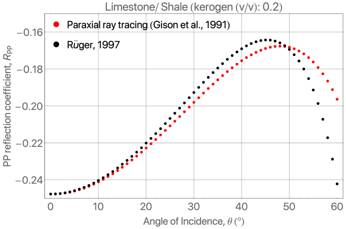

- How to overcome? Using Zoeppritz AVO inversion!

Zoeppritz equation in matrix form, [Zoeppritz, 1919]

$$\begin{bmatrix} R_{PP}(\theta_1) \\ R_{PS}(\theta_1) \\ T_{PP}(\theta_1) \\ T_{PS}(\theta_1) \end{bmatrix} = \begin{bmatrix} -\sin\theta_1 & -\cos\phi_1 & \sin\theta_2 & \cos\phi_2 \\ \cos\theta_1 & -\sin\phi_1 & \cos\theta_2 & -\sin\phi_2 \\ \sin 2\theta_1 & \frac{V_{P1}}{V_{S1}}\cos 2\phi_1 & \frac{\rho_2 V_{S2}^2 V_{P1}}{\rho_1 V_{S1}^2 V_{P2}}\cos 2\phi_1 & \frac{\rho_2 V_{S2} V_{P1}}{\rho_1 V_{S1}^2}\cos 2\phi_2 \\ -\cos 2\phi_1 & \frac{V_{S1}}{V_{P1}}\sin 2\phi_1 & \frac{\rho_2 V_{P2}}{\rho_1 V_{P1}}\cos 2\phi_2 & -\frac{\rho_2 V_{S2}}{\rho_1 V_{P1}}\sin 2\phi_2 \end{bmatrix}^{-1} \begin{bmatrix} \sin\theta_1 \\ \cos\theta_1 \\ \sin 2\theta_1 \\ \cos 2\phi_1 \end{bmatrix}$$

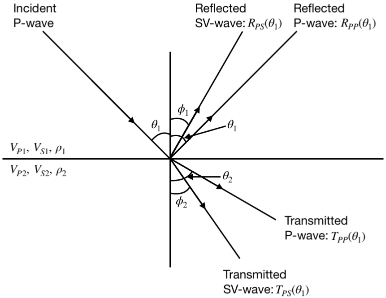

- Six parameters: V_{P1}, V_{P2}, V_{S1}, V_{S2}, ρ_1, and ρ_2
- Four angles: θ_1, θ_2, ϕ_1, and ϕ_2
- Non-linear equations
- Reformulation of the Zoeppritz equation & Adjoint state technique

Reformulation of the full Zoeppritz equation [Lavaud et al., 1999]

[Lavaud et al., 1999] rewrote the full Zoeppritz equation in terms of following:

- Three contrast parameters: e_p, e_s, and e_d
- Average values: χ

The expressions are of the form:

$$\begin{aligned} e_p &= (\alpha_2^2 - \alpha_1^2)/(\alpha_2^2 + \alpha_1^2) \\ e_s &= (\beta_2^2 - \beta_1^2)/(\beta_2^2 + \beta_1^2) \\ e_d &= (\rho_2 - \rho_1)/(\rho_2 + \rho_1) \\ \chi &= 2(\bar{\beta}^2)/(\bar{\alpha}^2) \end{aligned} \tag{2}$$

Effective implementation by reducing six (α_1, α_2, β_1, β_2, ρ_1 and ρ_2) to four parameters (e_p, e_s, e_d, and χ).

Method 1: Reformulation of the full Zoeppritz equation [Lavaud et al., 1999]

Exact PP-reflection coefficient:

$$R_{PP} = \frac{P - Q}{P + Q} \tag{3}$$

where variables P, Q, and other variables are functions of e_p, e_s, e_d, and χ described in Table 1.

Reformulation of the full Zoeppritz equation [Lavaud et al., 1999]

Table 1: Intermediate variables for equation 3.

$e = e_s + e_d$	$f = 1 - e_d^2$
$S_1 = \chi(1 + e_p)$	$S_2 = \chi(1 - e_p)$
$T_1 = \frac{2}{1-e_s}$	$T_2 = \frac{2}{1+e_s}$
$q^2 = S_1 \sin^2\theta$	$D = eq^2$
$M_1 = \sqrt{S_1 - q^2}$	$M_2 = \sqrt{S_2 - q^2}$
$N_1 = \sqrt{T_1 - q^2}$	$N_2 = \sqrt{T_2 - q^2}$
$A = e_d - D$	$K = D - A$
$B = 1 - K$	$C = 1 + K$
$Q = M_2(C^2 N_2 + fN_1) + 4q^2 A^2$	$P = M_1(B^2 N_1 + fN_2) + 4eDM_1 M_2 N_1 N_2$

Inverse problem as the minimization of a residual error function E

$$E(x) = \frac{1}{2}\sum_{i=1}^{N_{obs}} \| R_i^c{}_{PP}(x) - R_i^m{}_{PP} \|^2, \tag{4}$$

where

$R_i^m{}_{PP}$: Observed (measured) R_{PP} at θ_i

$R_i^c{}_{PP}$: Forward-modeled (computed) R_{PP} at θ_i

N_{obs}: Number of observations (θ_i)

x: Set of model parameters, e_p, e_s, e_d, and χ ($\therefore x \in \mathbb{R}^4$)

- Minimization of $E(x)$
- Computations of $\nabla_x E$: $\nabla_x R_{PP}$ [Lavaud et al., 1999, Lim et al., 2017]
- By applying adjoint state technique [Burger and Chavent, 1979]

Case Study: Avalon Shale

Model & Test Parameters

Upper Layer: Isotropic layer (known V_P, V_S, and ρ)
Lower Layer: Target VTI shale layer (unknown V_P, V_S, and ρ)

- Model based on Avalon shale from a vertical well in the Delaware basin.
- Limestone (Upper Layer) / Avalon shale (Lower Layer).
- Kerogen (v/v): 0, 0.1, 0.2, and 0.3.
- AVO data range: 0° - 20°, and 0° - 60°.

Data - Bone Spring/Avalon formation at Delaware basin

Well A: Vp (90°), Vs (90°), Vp (0°), Vs (0°), ρ, TOC for 122 data points.

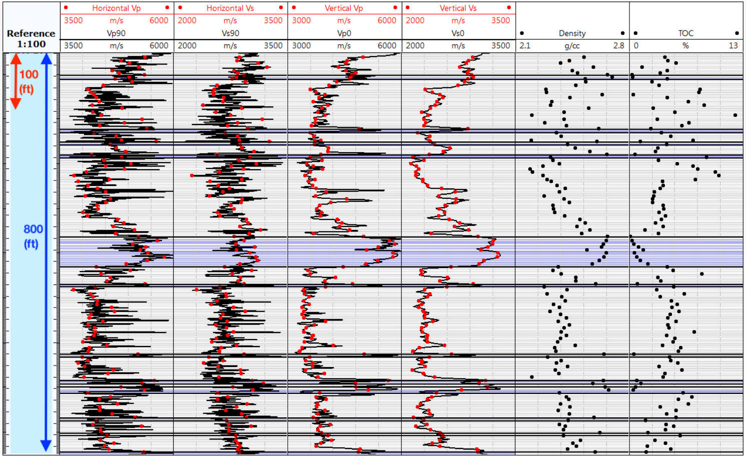

Provided by Chevron

Data: V_P, V_S, ρ, and Anisotropic AVO response w.r.t. organic richness

V_P (90°) & V_P (0°)

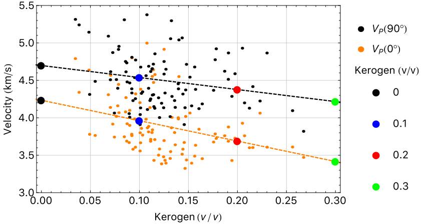

V_S (90°) & V_S (0°)

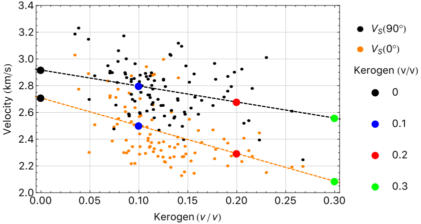

$\rho = -1.17 \cdot \textit{Kerogen} + 2.54$

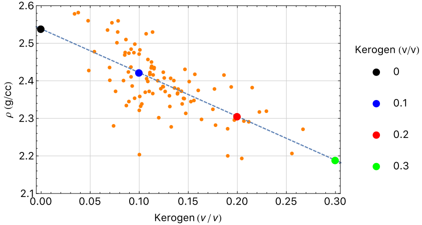

Anisotropic AVO response

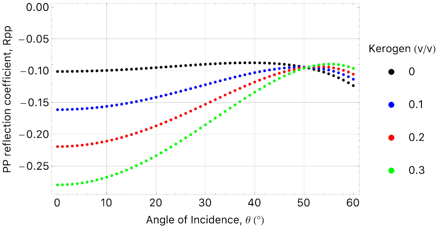

Inversion result: V_P, V_S, and ρ

V_P | V_S | ρ

AVO input ($0° \sim 20°$)

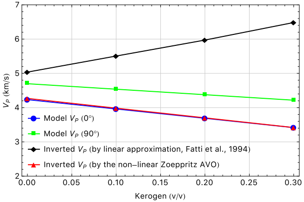

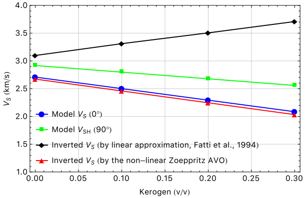

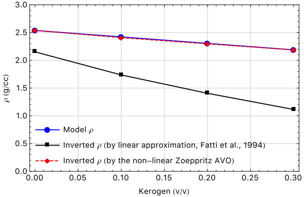

AVO input ($0° \sim 60°$)

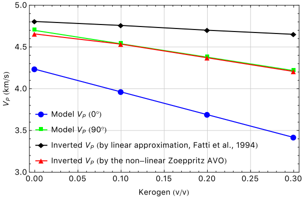

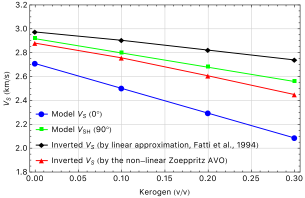

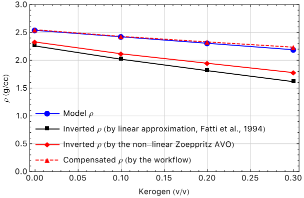

Summary of inversion results & Workflow to estimate seismic anisotropy

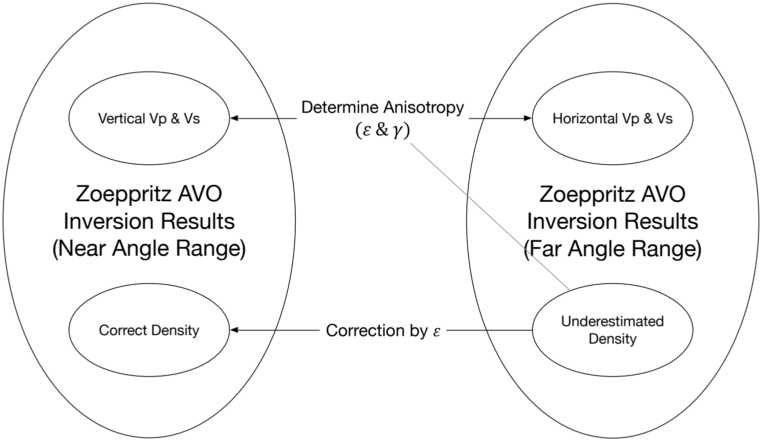

Estimation of seismic anisotropy (ϵ and γ)

Thomsen parameters (ϵ and γ) [Thomsen, 1986]:

$$
\begin{aligned}
\varepsilon &= \frac{c_{11} - c_{33}}{2c_{33}} = \frac{V_P^2(90^\circ) - V_P^2(0^\circ)}{2V_P^2(0^\circ)} \\
\gamma &= \frac{c_{66} - c_{44}}{2c_{44}} = \frac{V_{SH}^2(90^\circ) - V_S^2(0^\circ)}{2V_S^2(0^\circ)}
\end{aligned} \tag{5}
$$

where c_{ij} are elastic stiffness coefficient:

$$
\begin{aligned}
c_{11} &= \rho V_P^2(90^\circ) \\
c_{33} &= \rho V_P^2(0^\circ) \\
c_{44} &= \rho V_S^2(0^\circ) \\
c_{66} &= \rho V_{SH}^2(90^\circ) \\
c_{12} &= c_{11} - 2c_{66} \\
c_{13} &= -c_{44} + \sqrt{4\rho^2 V_P^4(45^\circ) - 2\rho V_P^2(45^\circ)(c_{11} + c_{33} + 2c_{44}) + (c_{11} + c_{44})(c_{33} + c_{44})}
\end{aligned} \tag{6}
$$

Estimation of seismic anisotropy (ϵ and γ)

ϵ

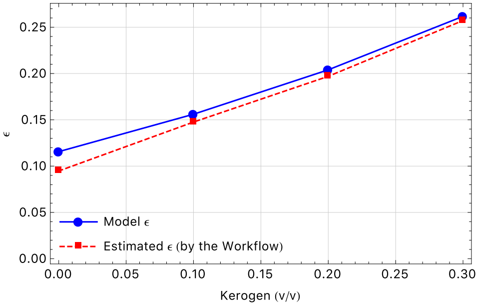

γ

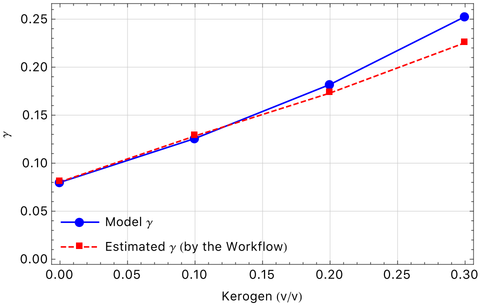

Estimation of geomechnical properties (E and ν)

Young's modulus and Poisson's ratio of VTI medium are expressed with elastic stiffness coefficients [King, 1964, Banik et al., 2012] as following:

$$
\begin{aligned}
E_V &= \frac{c_{33}(c_{11} - c_{66}) - c_{13}^2}{c_{11} - c_{66}} \qquad (= E_3) \\
E_H &= \frac{4c_{66}(c_{33}(c_{11} - c_{66}) - c_{13}^2)}{c_{11}c_{33} - c_{13}^2} \qquad (= E_1 = E_2) \\
\nu_V &= \frac{c_{13}}{2(c_{11} - c_{66})} \qquad (= \nu_{31} = \nu_{32}) \\
\nu_{HV} &= \frac{2c_{13}c_{66}}{c_{11}c_{33} - c_{13}^2} \qquad (= \nu_{13} = \nu_{23}) \\
\nu_{HH} &= \frac{c_{33}(c_{11} - 2c_{66}) - c_{13}^2}{c_{11}c_{33} - c_{13}^2} \qquad (= \nu_{12} = \nu_{21})
\end{aligned}
\tag{7}
$$

Estimation of geomechnical properties (E and ν)

E

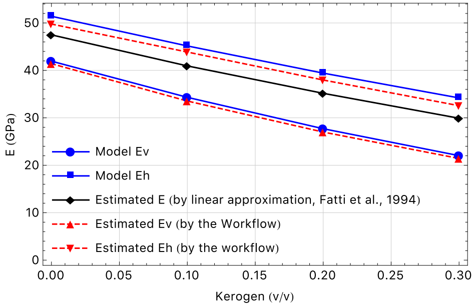

ν

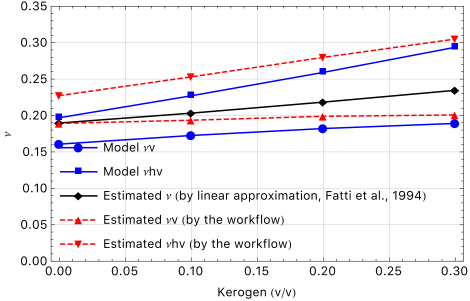

Estimation of TOC from density (by the workflow)

Why density for TOC estimation?

$$\rho = -1.17 \cdot \text{Kerogen} + 2.54$$

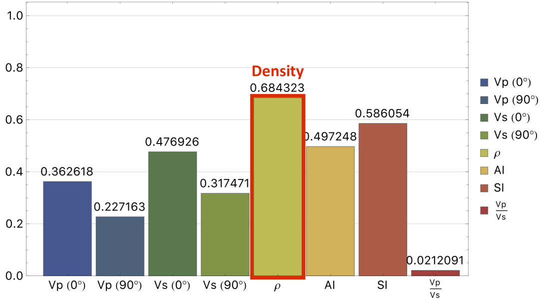

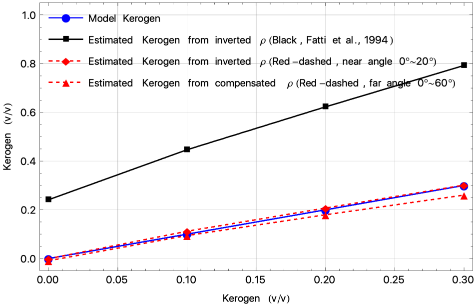

Conclusions

Conclusions

- Nonlinear Zoeppritz AVO inversion
  - Horizontal V_P, V_S, and underestimated ρ (with far AVO angle range)
  - Vertical V_P, V_S, and correct ρ (with near AVO angle range)

- Workflow to estimate
  - seismic anisotropy (ϵ and γ)
  - geomechnical properties (E and ν)
  - organic abundance (TOC)

- Potential Benefits & Business case of this research
  - Defining sweet spots for shale reservoirs in terms of 'fracability', 'completion' quality, and 'reservoir' quality
  - Optimization of well placement, and stimulated reservoir volume (SRV)

Acknowledgements

Chevron

- Funding and necessary data for this research were provided by Chevron through the Chevron Basin Modeling Center of Research Excellence (CBM CoRE) research program in the Berg-Hughes Center at Texas A&M University.

Theory [Lim et al., 2017]

Estimated Inversion Results

$$R_{PP}(\theta) = A + B\sin^2\theta + C\sin^2\theta\tan^2\theta. \tag{8}$$

[Rüger, 1997] (for Weak Anisotropy)

$$C = \frac{1}{2}\left[\frac{\Delta V_P(0^\circ)}{\bar{V}_P(0^\circ)} + \Delta\varepsilon\right] \tag{9}$$

[Wiggins et al., 1983] (for Isotropy)

$$C = \frac{1}{2}\frac{\Delta V_P}{\bar{V}_P}. \tag{10}$$

Comparison of C in equations 9 and 10 leads:

$$V_{P2}^{EST} \approx V_{P2}^{VTI}(90^\circ) + \frac{\left[V_{P1}^{ISO} - V_{P2}^{VTI}(90^\circ)\right]^2}{4V_{P1}^{ISO}}\varepsilon_2. \tag{11}$$

For small ε (weak anisotropy):

$$V_{P2}^{EST} \approx V_{P2}^{VTI}(90^\circ). \tag{12}$$

Estimated Inversion Results

$$R_{PP}(\theta) = A + B\sin^2\theta + C\sin^2\theta\tan^2\theta.$$

[Rüger, 1997] (for Weak Anisotropy)

$$A = \frac{1}{2}\frac{\Delta Z(0^\circ)}{\bar{Z}(0^\circ)} \qquad (13)$$

[Wiggins et al., 1983] (for Isotropy)

$$A = \frac{1}{2}\frac{\Delta Z}{\bar{Z}} = \frac{1}{2}\frac{\Delta(\rho V_P)}{(\rho \bar{V}_P)} \qquad (14)$$

Comparison of A in equations 13 and 14, and setting $V_{P2}^{EST} = V_{P2}^{VTI}(90^\circ)$ in equation 12 leads:

$$\rho_2^{EST} \approx \frac{V_{P2}^{VTI}(0^\circ)}{V_{P2}^{VTI}(90^\circ)}\rho_2^{VTI} = \frac{1}{1+\varepsilon_2}\rho_2^{VTI}. \qquad (15)$$

Supportive Supplementary Slides

V_P, V_S, and ρ from e_p, e_s, and e_d

$$
\begin{aligned}
V_{P2} &= \sqrt{\frac{1 + e_p}{1 - e_p}} \cdot V_{P1} \\
V_{S2} &= \sqrt{\frac{1 + e_s}{1 - e_s}} \cdot V_{S1} \\
\rho_2 &= \frac{1 + e_d}{1 - e_d} \cdot \rho_1
\end{aligned}
\tag{16}
$$

Sensitivity test for V_P with the model of Avalon shale

$0° \sim 20°$

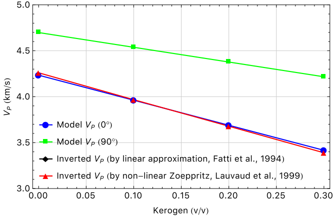

$0° \sim 23°$

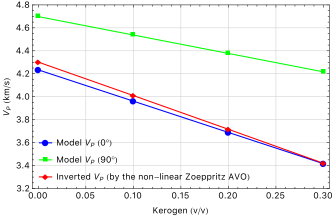

$0° \sim 26°$

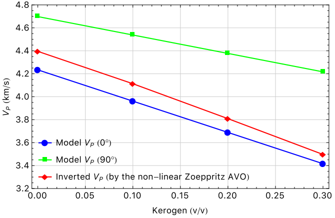

$0° \sim 29°$

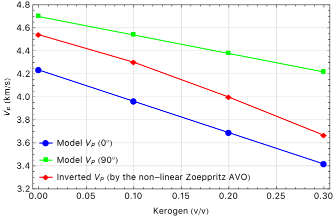

$0° \sim 32°$

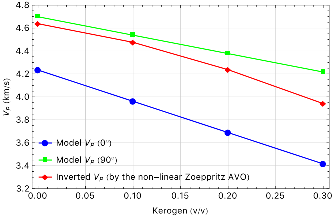

$0° \sim 35°$

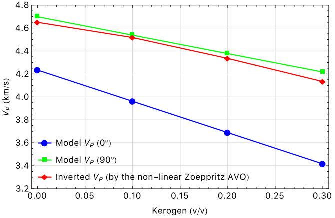

Sensitivity analysis to understand behavior of inversion results δ

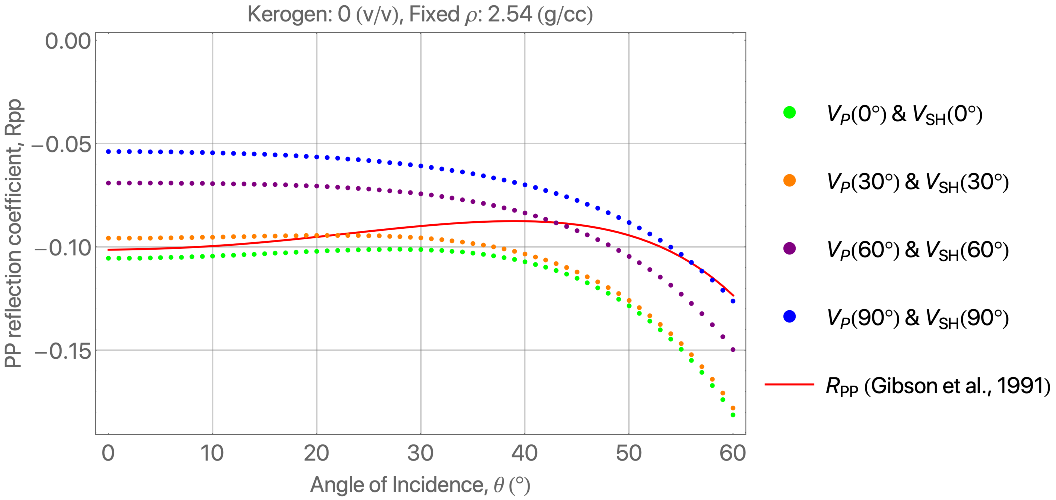

Test models for Avalon shale in Delaware basin

Table 2: Two-layer models for the testing AVO inversions

Model	Kerogen (v/v)	ρ (g/cm^3)	$V_P(0^\circ)$ (km/s)	$V_P(90^\circ)$ (km/s)	$V_S(0^\circ)$ (km/s)	$V_{SH}(90^\circ)$ (km/s)	ε	γ	δ
Upper Layer	0	2.63	5.05	5.05	2.90	2.90	0	0	0
Lower Layer	0●	2.54	4.23	4.70	2.71	2.92	0.12	0.08	0.06
	0.1●	2.42	3.96	4.54	2.50	2.80	0.16	0.13	0.08
	0.2●	2.31	3.69	4.38	2.29	2.68	0.20	0.18	0.10
	0.3●	2.19	3.42	4.22	2.09	2.56	0.26	0.25	0.12

Improvement by Joint Zoeppritz inversion [Lim et al., 2018]

$$E(m) = \frac{1}{2}\sum_{i=1}^{N}(\|R_i^d{}_{PP} - R_i^c{}_{PP}(m)\|^2 + \|R_i^d{}_{PS} - R_i^c{}_{PS}(m)\|^2), \quad (17)$$

where

R_i^d: Observed R_{PP} & R_{PS} at θ_i

R_i^c: Forward-modeled R_{PP} & R_{PS} at θ_i

N: Number of θ_i

m: Set of model parameters, e_p, e_s, e_d, and χ.

- Minimization of $E(m)$
- Computations of $\nabla E(m)$: ∇R_{PP} [Lavaud et al., 1999], ∇R_{PS} [Lim et al., 2018]
- By applying adjoint state technique [Burger and Chavent, 1979]